Application of the boson-expansion method to even Se and Ru isotopes

S. G. Lie and G. Holzwarth
Physik-Department der Technischen Universität München, Theoretische Physik, 8046 Garching b. München, Federal Republic of Germany
(Received 21 April 1975)

The expansion coefficients of a fourth-order collective Hamiltonian for the low-lying quadrupole vibrations are derived from the microscopic fermion Hamilton operator by a modified Marumori boson-expansion method. Their dependence on the phonon structure, on the parameters of the two-body (surface δ) interaction, and on the single-particle energies is numerically investigated. For the isotopes ^{76}Se, ^{78}Se and ^{100}Ru, ^{102}Ru the results are compared with coefficients that are obtained from phenomenological fits to low-lying levels. Quadrupole moments and $B(E2)$ values are calculated in lowest order.

[NUCLEAR STRUCTURE ^{76,78}Se, ^{100,102}Ru collective states microscopically by boson expansion.]

I. INTRODUCTION

The low-lying phonon states in spherical even-even nuclei still present a challenging problem to nuclear theory. The phenomenological collective model for quadrupole vibrations[1] predicts a first excited state with spin and parity 2^+, a triplet of two-phonon states at approximately twice the energy of the first with characters 0^+, 2^+, and 4^+, eventually followed by a three-phonon quintet (0^+, 2^+, 3^+, 4^+, 6^+) with strongly enhanced electric quadrupole matrix elements connecting members of different multiplets.

Nuclei following this pattern are found mainly in the medium weight region $50 < A < 150$. In lighter nuclei the single-particle features are too pronounced to allow pure slow collective vibrations, while the rapid onset of deformation in heavier open-shell nuclei leaves little space for isotopes that are soft enough for low-lying vibrations but not yet permanently deformed. The collective quadrupole motion appears to be best developed and well separated from single-particle motion for nuclei at least four protons and four neutrons (or four proton holes and four neutron holes) away from closed proton or neutron configurations. If there are only two particles or holes outside a single closed shell, two-particle (hole) states tend to interfere with the phonons and ought to be included explicitly into model calculations. Subshell closure ($Z = 40, N = 38, 56$) can be sensitively reflected in the vibrational pattern, especially if the other kind of particles are close to filling a major shell.[2]

These considerations leave about seven groups of isotopes as candidates for a description in terms of a purely collective oscillator Hamiltonian with small anharmonicities to account for the splitting of the multiplets and the deviations of transition matrix elements from the pure oscillator values: $^{72-78}_{32}$Ge, $^{74-80}_{34}$Se, $^{76-82}_{36}$Kr; $^{98-102}_{44}$Ru, $^{100-108}_{46}$Pd, $^{128-132}_{54}$Xe, and $^{132-134}_{56}$Ba. The first excited 0^+ state seems to be especially sensitive to the subshell closure at $N = 38$ (Ge, Se) and $Z = 40$ (Zr). For light Ge and Se isotopes model calculations therefore ought to include mechanisms for obtaining low-lying 0^+ states (e.g. pairing vibrations[3]).

The rotational band structure of nuclei with permanent quadrupole deformation in principle can be obtained from the collective quadrupole phonon model,[4-6] e.g. by increasing the third-order anharmonicities. This is possible and is so simple because the intrinsic structure of the phonon operator enters into the collective Hamiltonian only through the expansion coefficients, and these are determined by a phenomenological fit to the spectrum of a given nucleus. In a microscopic determination of the expansion coefficients, however, the intrinsic phonon structure must be allowed to change during the spherical-deformed transition, i.e., there has to be a self-consistent feedback from the calculated anharmonicities to the intrinsic structure of the phonon. Such a program, however, we do not intend in this paper and we will restrict our considerations to nuclei from the abovementioned groups of isotopes which are oscillating around an essentially spherical shape.

As in phenomenological approaches the physical meaning of the phonon operators need not be specified, there is a lot of freedom in choosing the model Hamiltonian. The simplest versions[7-9] assume a fourth-order coupling term diagonal in the phonon number. This then requires an expan-

sion of the transition operators up to third order.[7] The remaining freedom in the Hamiltonian (three parameters, apart from a scale) seems to be sufficient to describe the positions of the highest angular momentum members of the different phonon multiplets with good accuracy. Most of the other low-lying members, however, cannot be reproduced by such simple Hamiltonians. (E.g., for degenerate 2^+ and 4^+ two-phonon states the model predicts degeneracy of the 0^+, 3^+, 4^+, and 6^+ members of the quintet. This is in strong contradiction with a case like ^{102}Ru where the complete quintet seems to be present.) Furthermore, a Hamiltonian diagonal in the phonon number implies a very complicated microscopic structure of the phonon, containing not only two-quasiparticle components, but also large four-, six-, etc., quasiparticle components, meaning that the problem of anharmonicities has to be solved essentially in the fermion space. An alternative approach specifies the physical meaning of the phonon, for example by assuming a rapidly converging expansion of the quadrupole operator in powers of the phonon operators (usually only the linear term is kept).[6,10,11] The fourth-order Hamiltonian then contains all possible off-diagonal terms with altogether seven parameters (apart from a scale).

The number of parameters may be reduced by formally dividing the Hamiltonian into potential and kinetic energy parts $V(Q)+T(P,Q)$ and requiring the kinetic energy T to be of the form $P^2/2M$, with M as constant inertia parameter. This leads to simple relations between the parameters for diagonal and off-diagonal terms of a given order in the phonon Hamiltonian.[5] It is an interesting question whether it is necessary to introduce sixth-order terms into the potential $V(Q)$ while omitting fourth-order terms like P^2Q^2 or P^4, as sixth-order terms can introduce triaxial minima into the potential energy surface while fourth-order terms cannot.[12]

Phenomenological fits of the most general fourth-order ansatz to experimental spectra tend to produce general similarities in the ratios between diagonal and off-diagonal terms which will be discussed in Sec. II. It is the main aim of this paper to investigate whether these features can be obtained from a genuinely microscopic approach to the anharmonicities in vibrational nuclei. The most appropriate means to construct the collective Hamiltonian on a microscopic basis seems to be the boson-expansion method.[13-15] These expansions originally have been formulated in terms of pure quasiparticle operators[13,15] or two quasiparticle states[14] where their convergence may be quite poor. It has been demonstrated in solvable models[16,17] that the convergence of these expansions is excellent if they are formulated from the very beginning in terms of the *collective* operators (or collective states). This can be done very easily in the case of Marumori's expansion. The only additional difficulty arising is that the normalization constants of many-phonon states in fermion space have to be calculated. From Ref. 16 it can be seen that this approach is definitely superior to Sørensen's expansion (in that model). These arguments led us to make use of Marumori's expansion modified in the above sense to derive the collective Hamiltonian. The details are given in Sec. III.

An important question is how strongly the precise structure of the phonon operator enters into the resulting anharmonicities. For comparison we use a schematic phonon and the collective solution of the Tamm-Dancoff equations. The random-phase approximation (RPA) in most cases does not lead to stable solutions and cannot be used as a starting basis. The backward going graphs, however, show up for Tamm-Dancoff phonons in second-order off-diagonal terms of the boson expansion, and there they are easily taken into account because the fourth-order terms restore the stability of the collective motion.

The dependence of the resulting anharmonicities on the phonon structure, the parameters of the surface δ two-body interaction, the single-particle energies, and the particle number is numerically investigated in Sec. IV. For four isotopes we present a detailed comparison of the microscopically determined expansion coefficients with phenomenological fits to the experimental level scheme.

II. ANHARMONIC VIBRATOR MODEL

We have selected four different nuclei, the Se isotopes ^{76}Se and ^{78}Se and two Ru isotopes ^{100}Ru and ^{102}Ru, which we consider to be favorable examples for a description in terms of an anharmonic vibrator Hamiltonian containing only the collective quadrupole degree of freedom. The phenomenological model Hamiltonian is taken as

$$H_{\rm coll}=\tfrac{1}{2}E_0+\tfrac{1}{2}h_{11}[B^\dagger B]_0+h_{20}[B^\dagger B^\dagger]_0+h_{30}[[B^\dagger B^\dagger]_2 B^\dagger]_0+h_{21}[[B^\dagger B^\dagger]_2 B]_0+h_{40}[B^\dagger B^\dagger]_0[B^\dagger B^\dagger]_0$$
$$+h_{31}[B^\dagger B^\dagger]_0[B^\dagger B]_0+\sum_{J=0,2,4}\tfrac{1}{2}h_{22}^{(J)}[[B^\dagger B^\dagger]_J[BB]_J]_0+\text{h.c.} \qquad (1)$$

The operators $B^\dagger$ create bosons with angular momentum 2, and the brackets indicate angular momentum coupling. Without introducing higher-order terms, the h_{20} part can always be eliminated by a unitary transformation and therefore can be omitted. Apart from the uninteresting constant E_0 and a common scale factor (e.g. h_{11}), this Hamiltonian contains seven independent parameters which can be fitted to obtain the eight triplet plus quintet members of the phonon spectrum of a given nucleus. In three of the four isotopes mentioned above only seven states are known (only in ^{102}Ru the quintet is complete), therefore the missing quintet member is tentatively predicted from the fits. The resulting wave functions then can be used to calculate matrix elements of transition operators. In lowest order the quadrupole operator is taken as

$$Q_{2M} = t(B^\dagger_{2M} + (-)^M B_{2-M}) \ . \tag{2}$$

In this approximation ratios of $B(E2)$ values then are parameter free. In previous work[11,18] we have pointed out that it is advantageous to start the fitting procedure from the following relations:

$$h_{21}/h_{30} = 3, \quad h_{31}/h_{40} = 4 \ , \tag{3a}$$

$$h^{(0)}_{22}/h_{40} = 2.8, \quad h^{(2)}_{22}/h_{40} = 1.8, \quad h^{(4)}_{22}/h_{40} = 2.4 \ , \tag{3b}$$

These relations follow[5] from a collective Hamiltonian which contains a kinetic energy quadratic in $P \propto i(B^\dagger - B)$ with a constant inertia parameter, and a potential up to fourth order in $Q \propto (B^\dagger + B)$. It turned out that satisfactory fits can be obtained while keeping the ratios (3a) fixed or close to the starting values. However, satisfactory fits in most cases can only be reached with the ratios (3b) differing appreciably from the starting values; especially the $h^{(2)}_{22}$ coefficient tends to be quite small and even negative (cf. e.g. the three Kr isotopes[18]: ^{78}Kr, ^{80}Kr, ^{82}Kr, and ^{102}Ru [11]). In Figs. 1–4 we compare the experimental spectra with the lowest eigenvalues of the Hamiltonian (1); the fitted coefficients $r_{ij} = h_{ij}/h_{11}$ are given in Table I. Rewriting the Hamiltonian (1) in terms

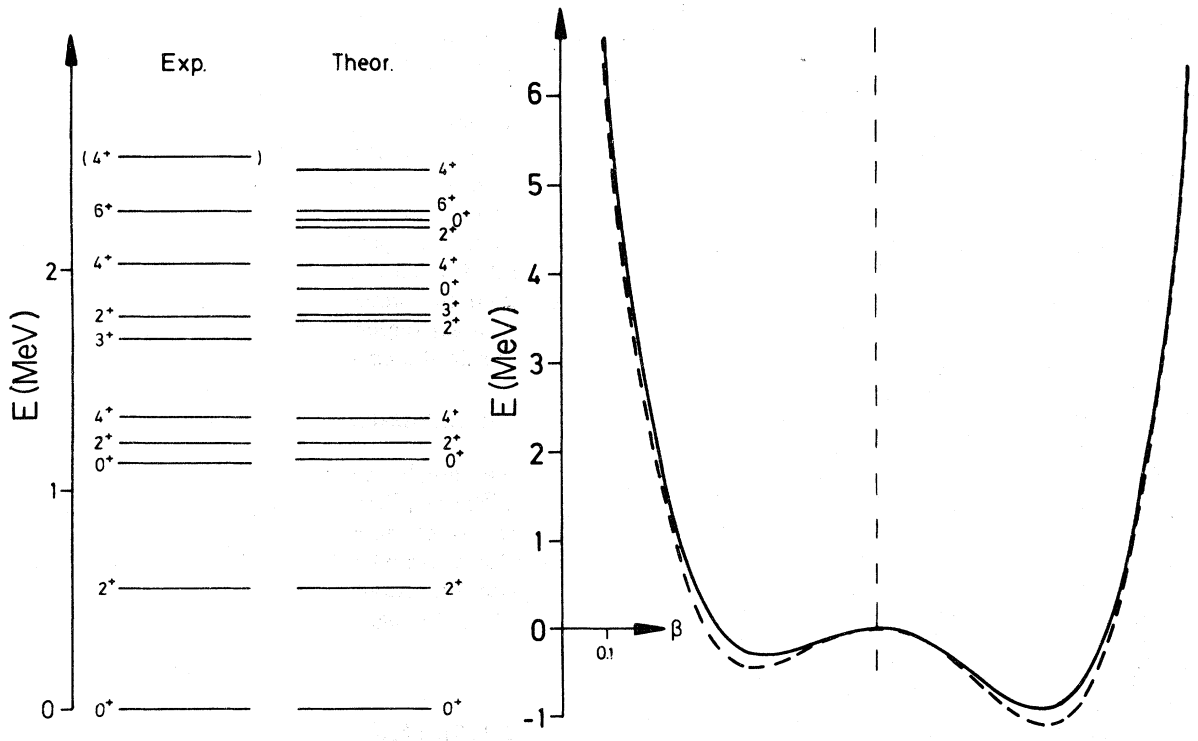

FIG. 1. The experimental energy levels (Ref. 29) of ^{76}Se as compared to the eigenvalues of the collective Hamiltonian (1) with the fitted coefficients given in Table I. The full curve shows the corresponding potential energy in the intrinsic β-γ frame for $\gamma = 0°$. The dashed curve is the potential resulting from the microscopic calculation.

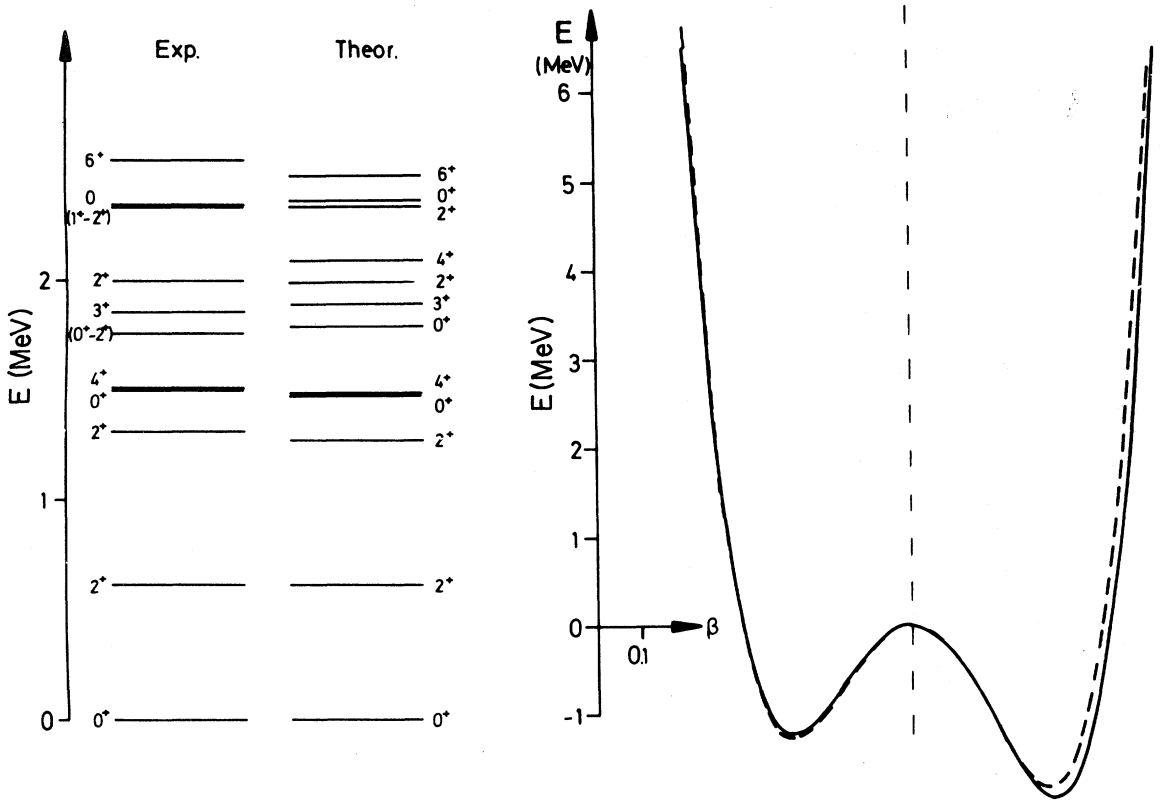

FIG. 2. Energy levels (Ref. 30) and potential energy for ^{78}Se. See caption of Fig. 1.

of Q and P leads to a separation of H into kinetic and potential energy parts $T(P, Q) + V(Q)$.[11] The potential energy $V(Q)$, transformed into the intrinsic β-γ frame, is plotted in Figs. 1–4 for the different nuclei along the $\gamma = 0°$ axis. Evidently all four isotopes display a maximum for the potential at zero deformation implying that an RPA approach for the phonons would fail. The quality of agreement for the $B(E2)$ values and the quadrupole moments is presented in Tables II–IV. Of course one might try harder than we did here to obtain even better agreement for the energies with slightly changed coefficients r_{ij}, but the over-all features of the transition probabilities remain essentially the same; and, in any case, one should not try to push this simple model too far. Our main aim in the following sections will be to try whether one can obtain the general pattern for the coefficients r_{ij} which results from these fits from a boson expansion of the microscopic fermion Hamiltonian for these nuclei.

III. MICROSCOPIC DERIVATION OF THE EXPANSION COEFFICIENTS

As outlined in the Introduction, we shall use a modified Marumori expansion to construct the collective Hamiltonian on a microscopic basis. The original Marumori transformation[14] from the fermion space to the space of ideal bosons is defined in terms of antisymmetric operators $B^\dagger_{\mu\nu}$, satisfying the Bose commutation relations

$$[B_{\mu\nu}, B^\dagger_{\rho\sigma}] = \delta_{\mu\rho}\delta_{\nu\sigma} - \delta_{\mu\sigma}\delta_{\nu\rho} \tag{4}$$

and the antisymmetry requirement

$$B^\dagger_{\mu\nu} = -B^\dagger_{\nu\mu} . \tag{5}$$

The index pair $\mu\nu$ corresponds to the indices μ, ν of a two-quasiparticle operator $b^\dagger_\mu b^\dagger_\nu$ in the space of fermions. Writing $|0\rangle$ and $|0)$ for the vacua of fermions and bosons, respectively, the transformation is given by

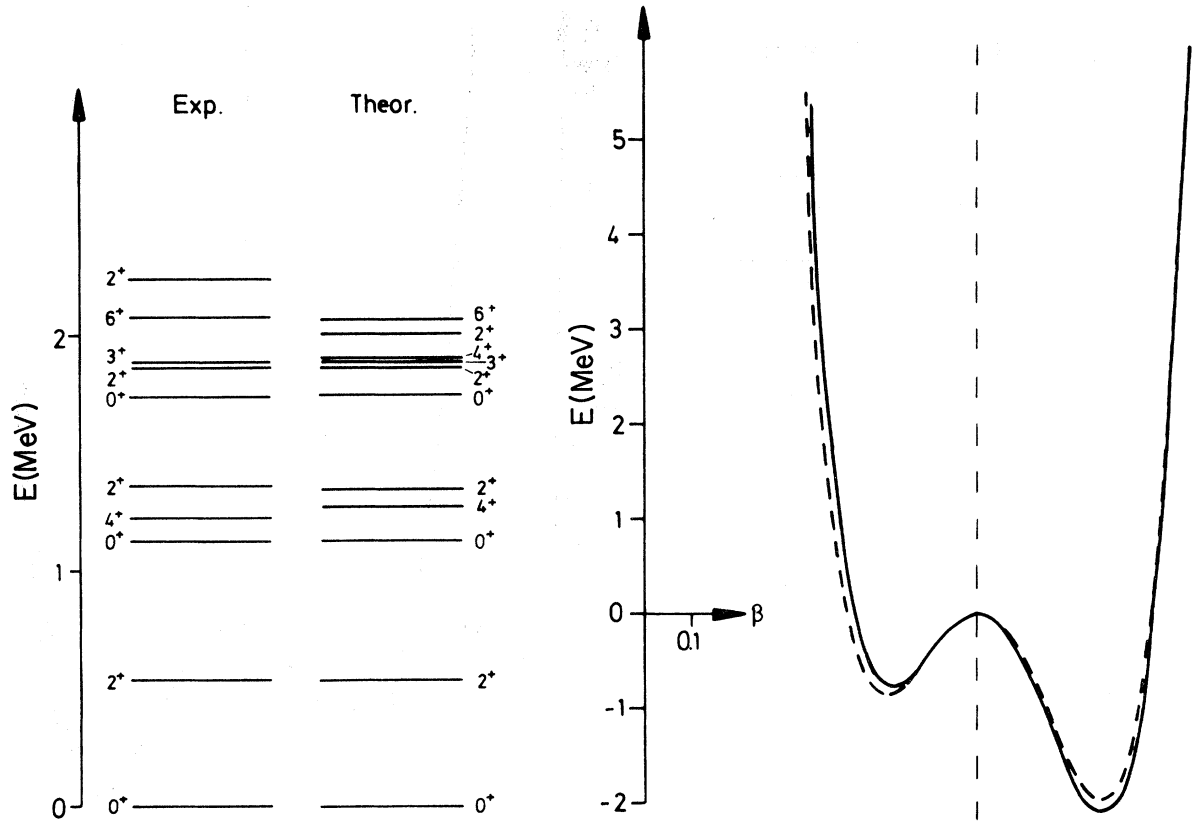

FIG. 3. Energy levels (Ref. 29) and potential energy for ^{100}Ru. See caption of Fig. 1.

$$U=\sum_n \frac{1}{(2n)![(2n-1)!!]^{1/2}} \sum_{\mu_1\nu_1\cdots\mu_n\nu_n} \sum_{\mathcal{P}} (-)^{\mathcal{P}} (B^\dagger_{\mu_1\nu_1}\cdots B^\dagger_{\mu_n\nu_n})|0\rangle\langle 0|\, b_{\nu_n} b_{\mu_n}\cdots b_{\nu_1} b_{\mu_1} \tag{6}$$

with $\mathcal{P}$ denoting all possible permutations of the $\{\mu_i\}$. Using for the projector on the boson vacuum the identity

$$|0)(0| =: \exp\left(-\tfrac{1}{2}\sum_{\mu\nu} B^\dagger_{\mu\nu} B_{\mu\nu}\right): \tag{7}$$

the image O_B of any fermion operator O_F in the boson space is then obtained as an infinite normal-ordered power series in terms of the operators $B^\dagger_{\mu\nu}$ and $B_{\mu\nu}$:

$$O_B = U O_F U^\dagger . \tag{8}$$

A natural way to obtain a collective Hamiltonian for phonons which are linear superpositions of two-quasiparticle operators

$$A^\dagger_i = \sum_{\mu\nu} c^{(i)}_{\mu\nu} b^\dagger_\mu b^\dagger_\nu \tag{9}$$

and, correspondingly, for the bosons

$$B^\dagger_i = \sum_{\mu\nu} c^{(i)}_{\mu\nu} B^\dagger_{\mu\nu}, \quad [B_i, B^\dagger_j] = \delta_{ij} \tag{10}$$

seems to be the following: Invert relations (10) by making use of the completeness of the coefficients $c^{(i)}_{\mu\nu}$

$$\sum_i c^{(i)*}_{\mu\nu} c^{(i)}_{\rho\sigma} = \tfrac{1}{4}(\delta_{\mu\rho}\delta_{\nu\sigma} - \delta_{\mu\sigma}\delta_{\nu\rho}) \tag{11}$$

to obtain

$$B^\dagger_{\mu\nu} = 2\sum_i c^{(i)*}_{\mu\nu} B^\dagger_i \tag{12}$$

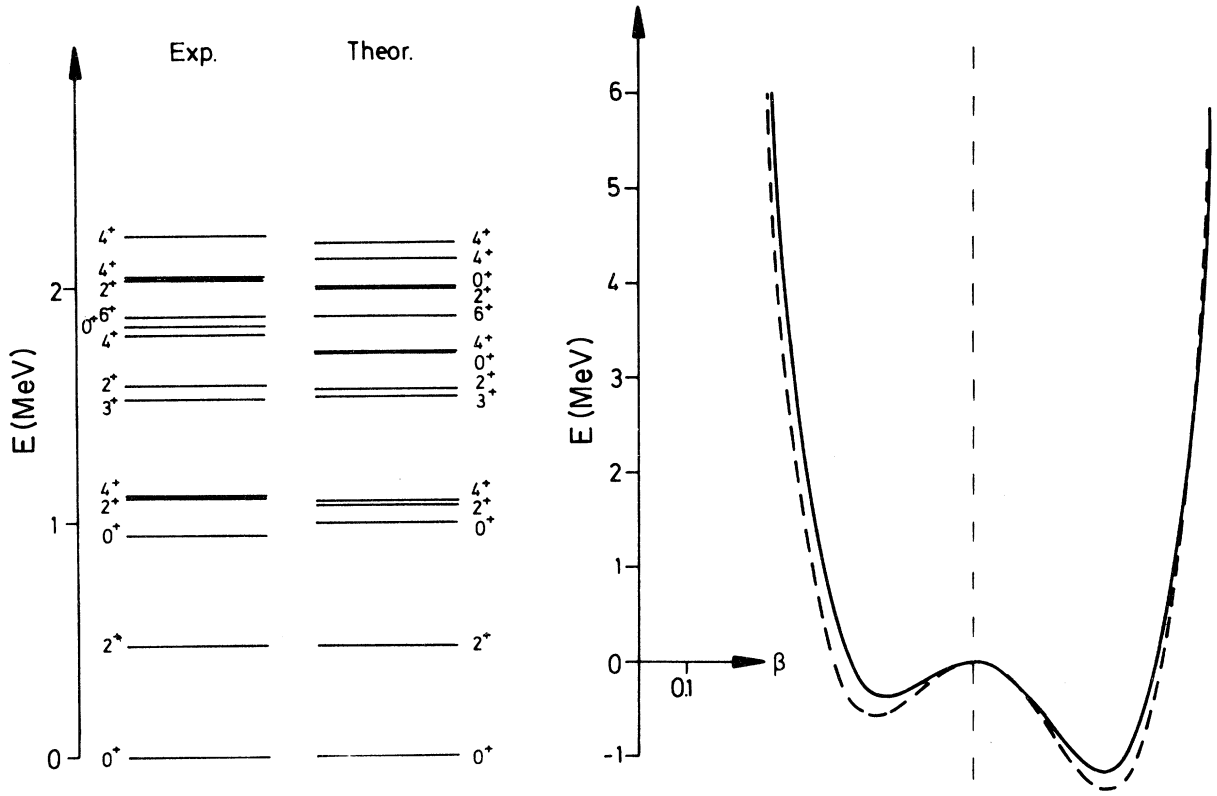

FIG. 4. Energy levels (Refs. 29 and 30) and potential energy for ^{102}Ru. See caption of Fig. 1.

and then insert this into the transformation (6):

$$U=\sum_n \frac{2^n[(2n-1)!!]^{1/2}}{(2n)!} \times \sum_{i_1\cdots i_n} B^\dagger_{i_1}\cdots B^\dagger_{i_n}|0\rangle\langle 0|A_{i_n}\cdots A_{i_1} .$$

As long as the *complete* sums over the indices i are performed, this transformation still is identical with Eq. (6) although the states $A^\dagger_{i_1}\cdots A^\dagger_{i_n}|0\rangle$ are neither orthogonal nor normalized no longer. However, usually one will truncate the i sums to include only the interesting collective modes ($i=0$, say), and then obtain

$$U=\sum_n \frac{2^n[(2n-1)!!]^{1/2}}{(2n)!}(B^\dagger_0)^n|0\rangle\langle 0|(A_0)^n . \quad (13)$$

This, however, obviously no longer is a meaningful and unitary transformation, because neither the fermion nor the boson states are correctly normalized.

Instead, if one wants to establish a transformation similar to Eq. (6) in the subspace of collective phonons *only*, one has to put up the operator U directly in terms of normalized multiphonon states and not try to start from Eq. (6). That is, we write

$$U=\sum_n N^B_n(B^\dagger_0)^n|0\rangle\langle 0|(A_0)^n N^F_n \quad (14)$$

TABLE I. The coefficients r_{ij} resulting from phenomenological fits to the low-lying levels of Se and Ru isotopes.

	r_{21}	r_{30}	$r^{(0)}_{22}$	$r^{(2)}_{22}$	$r^{(4)}_{22}$	r_{31}	r_{40}
^{76}Se	0.278	0.062	0.192	0.028	0.375	0.389	0.070
^{78}Se	0.212	0.071	0.277	0.189	0.526	0.605	0.115
^{100}Ru	0.385	0.128	0.254	0.161	0.386	0.580	0.125
^{102}Ru	0.332	0.111	0.237	0.049	0.349	0.480	0.120

TABLE II. Comparison between experimental (Refs. 30–33) and theoretical ratios of $B(E2)$ values.

	^{76}Se		^{78}Se		^{100}Ru		^{102}Ru	
	$B(E2)/B'(E2)$		$B(E2)/B'(E2)$		$B(E2)/B'(E2)$		$B(E2)/B'(E2)$	
$J_i^\pi \to J_f^\pi / J_i'^\pi \to J_f'^\pi$	Theo.	Exp.	Theo.	Exp.	Theo.	Exp.	Theo.	Exp.
$0_2^+ \to 2_1^+ / 2_1^+ \to 0_1^+$	1.011	0.919	0.545		0.479	1.0	0.956	
$2_2^+ \to 0_1^+ / 2_2^+ \to 2_1^+$	0.060	0.031	0.016	0.030	0.045	0.066	0.081	0.055
$4_1^+ \to 2_1^+ / 2_1^+ \to 0_1^+$	1.731	1.979	1.554		1.635	1.3	1.712	1.408
$0_3^+ \to 2_1^+ / 0_3^+ \to 2_2^+$	0.122		0.094		0.616		0.035	0.160
$3_1^+ \to 2_1^+ / 3_1^+ \to 2_2^+$	0.087		0.024	0.025	0.043		0.061	0.028
$3_1^+ \to 2_1^+ / 3_1^+ \to 4_1^+$	0.351		0.074		0.213		0.349	0.170
$2_3^+ \to 0_1^+ / 2_3^+ \to 2_1^+$	85.3		1.462	0.33	1.809		1.538	1.10
$2_3^+ \to 0_1^+ / 2_3^+ \to 0_2^+$	0.013		0.015		0.061		0.005	0.003
$2_3^+ \to 0_1^+ / 2_3^+ \to 2_2^+$	0.060		0.189	0.009	0.063		0.021	
$2_3^+ \to 0_1^+ / 2_3^+ \to 4_1^+$	0.031		0.072		0.099		0.012	
$4_2^+ \to 2_1^+ / 4_2^+ \to 2_2^+$	0.037		0.007		22.4		0.020	0.007
$4_2^+ \to 2_1^+ / 4_2^+ \to 4_1^+$	0.060		0.009		1.137		0.039	0.013
$6_1^+ \to 4_1^+ / 2_1^+ \to 0_1^+$	2.14		1.803		1.477		2.049	

with

$$(0|\, B_0^n B_0^{\dagger m}|\, 0) = \delta_{nm}(N_n^B)^{-2}\ , \qquad (15)$$

$$\langle 0|\, A_0^n A_0^{\dagger m}|\, 0\rangle = \delta_{nm}(N_n^F)^{-2}\ .$$

A similar difficulty ought to appear in the Beliaev-Zelevinsky method which also starts out from two-quasiparticle operators, then is transformed into the i representation Eqs. (9) and (10) before being truncated to the collective branches. Investigations of this point are in progress[19] and are especially interesting because the BZ method allows a summation of the infinite boson series in terms of square roots.[20]

We restrict the following considerations to

TABLE III. Comparison between experimental (Refs. 30–33) and theoretical $B(E2)$ values; [$B(E2,\ 2_1 \to 0_1)$ normalized].

	^{76}Se		^{78}Se		^{100}Ru		^{102}Ru	
	$B(E2)$ (s.p.u.)		$B(E2)$ (s.p.u.)		$B(E2)$ (s.p.u.)		$B(E2)$ (s.p.u.)	
$J_i^\pi \to J_f^\pi$	Theo.	Exp.	Theo.	Exp.	Theo.	Exp.	Theo.	Exp.
$2_1^+ \to 0_1^+$	49.6	49.6	35.6	35.6	41.4	41.4	50.4	50.4
$0_2^+ \to 2_1^+$	50.2	45.6	19.4		19.8	41.7	49.9	
$2_2^+ \to 2_1^+$	50.3	34.0	37.6	33.8	29.4	24.3	36.0	25.9
$2_2^+ \to 0_1^+$	3.03	1.05	0.687	1.01	1.3	1.6	2.9	1.43
$4_1^+ \to 2_1^+$	85.9	98.2	55.3		67.7	52.9	89.4	71.0
$0_3^+ \to 2_2^+$	47.1		29.7		14.5		34.7	
$3_1^+ \to 2_2^+$	64.8		44.8		15.5		75.8	
$2_3^+ \to 0_2^+$	39.3		19.9		19.4		45.3	
$4_2^+ \to 2_2^+$	49.0		31.2		0.014		44.7	
$6_1^+ \to 4_1^+$	106.1		64.2		61.2		106.9	

quadrupole phonons

$$A^{\dagger}_{2M} = \sum_{\alpha\beta} c_{\alpha\beta,2M} b^{\dagger}_{\alpha} b^{\dagger}_{\beta} = \sum_{ab} c_{ab,2} [b^{\dagger}_{a} b^{\dagger}_{b}]_{2M} , \quad (16)$$

where the bracket again indicates angular-momentum coupling and $\alpha = \{n_\alpha, l_\alpha, j_\alpha, m_\alpha, \tau_{3\alpha}\}$, $a = \{n_\alpha, l_\alpha, j_\alpha, \tau_{3\alpha}\}$ denote the quantum numbers of the single fermion levels. We take the coefficients $c_{ab,2}$ diagonal in the third component of the isospin and in the following we will omit the index 2 at the phonon operator $A^{\dagger}_2$ and the coefficients $c_{ab,2}$. For the expansion of the Hamiltonian up to fourth order we shall need the operator U (14) up to the three phonon states:

TABLE IV. Theoretical values for the static quadrupole moments (only relative signs are determined by the theory).

J^{π}_i	^{76}Se Q (eb)	^{78}Se Q (eb)	^{100}Ru Q (eb)	^{102}Ru Q (eb)
2^+_1	−0.471	−0.283	−0.560	−0.673
2^+_2	+0.377	+0.248	+0.355	+0.563
4^+_1	−0.688	−0.390	−0.743	−0.933
2^+_3	−0.390	−0.238	−0.290	−0.339
4^+_2	−0.073	+0.047	−0.564	−0.320
6^+_1	−0.931	−0.440	−1.077	−1.294

$$U = |0\rangle\langle 0| + \sum_{M} |1,2M\rangle\langle 1,2M| + \sum_{\substack{J=0,2,4 \\ M}} |2,JM\rangle\langle 2,JM| + \tfrac{1}{3} \sum_{\substack{J=0,2,4 \\ M}} |3,2(J)M\rangle\langle 3,2(J)M| \quad (17)$$

with

$$\begin{aligned} |1,2M\rangle &= N^B_1 B^{\dagger}_M |0\rangle , & |1,2M\rangle &= N^F_1 A^{\dagger}_M |0\rangle , \\ |2,JM\rangle &= N^B_{2J} [B^{\dagger} B^{\dagger}]_{JM} |0\rangle , & |2,JM\rangle &= N^F_{2J} [A^{\dagger} A^{\dagger}]_{JM} |0\rangle , \\ |3,2(J)M\rangle &= N^B_{3(J)} [[B^{\dagger} B^{\dagger}]_J B^{\dagger}]_{2M} |0\rangle , & |3,2(J)M\rangle &= N^F_{3(J)} [[A^{\dagger} A^{\dagger}]_J A^{\dagger}]_{2M} |0\rangle . \end{aligned} \quad (18)$$

The microscopic fermion Hamiltonian

$$H = \sum_{\alpha\beta} t_{\alpha\beta} a^{\dagger}_{\alpha} a_{\beta} + \tfrac{1}{4} \sum_{\alpha\beta\gamma\delta} V_{\alpha\beta\gamma\delta} a^{\dagger}_{\alpha} a^{\dagger}_{\beta} a_{\delta} a_{\gamma} \quad (19)$$

is rewritten in terms of BCS quasiparticle operators $b^{\dagger}_{\alpha} = u_\alpha a^{\dagger}_{\alpha} + v_\alpha a_{\bar{\alpha}}$:

$$H' = H - \lambda \hat{N} = H_{00} + H_{11} + H_{20} + H_{22} + H_{31} + H_{40} , \quad (20)$$

where H_{ij} denote the terms containing i quasiparticle creation (annihilation) operators and j annihilation (creation) operators. Transforming this Hamiltonian H into the boson space by means of the transformation U (14)

$$H_{\rm coll} = UHU^{\dagger} = UH'U^{\dagger} + \lambda U \hat{N} U^{\dagger} , \quad (21)$$

we obtain $H_{\rm coll}$ in the form (1) with the coefficients

h_{ij} given by the following reduced matrix elements:

$$\begin{aligned} E_0 &= \langle 0 \| H \| 0 \rangle , \\ h_{11} &= \langle 1,2 \| H \| 1,2 \rangle - \sqrt{5}\, \langle 0 \| H \| 0 \rangle = \langle 1,2 \| H_{11} + H_{22} \| 1,2 \rangle , \\ h_{20} &= \langle 2,0 \| H \| 0 \rangle / \sqrt{2!} = \langle 2,0 \| H_{40} \| 0 \rangle / \sqrt{2!} , \\ h_{21} &= \langle 2,2 \| H \| 1,2 \rangle / \sqrt{2!} = \langle 2,2 \| H_{31} \| 1,2 \rangle / \sqrt{2!} , \\ h_{31} &= \sqrt{\tfrac{5}{14}}\, (\langle 3,2(0) \| H \| 1,2 \rangle - \sqrt{14}\, h_{20}) \\ &= \sqrt{\tfrac{5}{14}}\, (\langle 3,2(0) \| H_{40} \| 1,2 \rangle - \sqrt{14}\, h_{20}) , \\ h^{(J)}_{22} &= [(2J+1)^{1/2}/2!]\, (\langle 0 \| H \| 0 \rangle - 2! \langle 1,2 \| H \| 1,2 \rangle / \sqrt{5}) + \langle 2,J \| H \| 2,J \rangle / 2! \\ &= (1/2!) \{ \langle 2,J \| H_{11} + H_{22} \| 2,J \rangle - [(2J+1)/5]^{1/2} h_{11} \} , \\ h_{30} &= h_{40} = 0 . \end{aligned} \quad (22)$$

In the Eqs. (22) we have omitted the second term of Eq. (21) because it essentially contributes only two constants λN for protons and neutrons, respectively. The explicit expressions for the expansion coefficients h_{ij} and the normalization constants N_n^B and N_n^F in terms of the amplitudes c_{ab}, the matrix elements of the two-body force $V_{\alpha\beta\gamma\delta}$, and the BCS occupation amplitudes u_α and v_α are given in the Appendix A.

Phonons of the form (16) lead to vanishing coefficients h_{30} and h_{40} because the Hamiltonian (20) contains only terms of at most four fermion creation or annihilation operators. On the other hand, the coefficient h_{20} in Eq. (22) generally does not vanish, but turns out to be of the same order of magnitude as the diagonal h_{11} term. In fact, for the nuclei considered here the absolute value of h_{20} is slightly larger than $\frac{1}{2}h_{11}$ meaning that the motion in the direction of the collective degree of freedom is unstable (in second order) in agreement with the phenomenological results of Sec. II. To make it evident how the higher-order terms restore the stability and to be able to compare directly with the results of Sec. II, we introduce a new boson operator by the unitary transformation

$$\tilde{B}_M^\dagger = xB_M^\dagger + y(-)^M B_{-M} \tag{23}$$

with x and y satisfying the unitarity relation

$$x^2 - y^2 = 1 \ . \tag{24}$$

Rewriting the boson Hamiltonian in terms of the operators (23) now introduces nonvanishing $\tilde{h}_{30}[[\tilde{B}^\dagger\tilde{B}^\dagger]_2\tilde{B}^\dagger]_0$ and $\tilde{h}_{40}[\tilde{B}^\dagger\tilde{B}^\dagger]_0[\tilde{B}^\dagger\tilde{B}^\dagger]_0$ terms. The relations between the new coefficients $\tilde{h}_{ij}$ and the original h_{ij} from Eqs. (22) are

$$\begin{aligned}
\tilde{h}_{11} &= (x^2+y^2)h_{11} + 4xyh_{20} + \frac{14}{\sqrt{5}}xy(x^2+3y^2)h_{31} + \frac{56}{\sqrt{5}}x^2y^2h_{40} + \frac{4}{\sqrt{5}}y^2\sum_{J=0,2,4}[5\delta_{J0}x^2 + \hat{J}(x^2+y^2)]h_{22}^{(J)} \ , \\
\tilde{h}_{20} &= xyh_{11} + (x^2+y^2)h_{20} + \frac{7}{\sqrt{5}}y^2(3x^2+y^2)h_{31} \\
&\quad + \frac{14}{\sqrt{5}}xy(x^2+y^2)h_{40} + \frac{1}{\sqrt{5}}xy\sum_{J=0,2,4}[5\delta_{J0}(x^2+y^2) + 4\hat{J}y^2]h_{22}^{(J)} \ , \\
\tilde{h}_{21} &= 3xy(x+y)h_{30} + (x^3+2x^2y+2xy^2+y^3)h_{21} \ , \\
\tilde{h}_{30} &= (x^3+y^3)h_{30} + xy(x+y)h_{21} \ , \\
\tilde{h}_{31} &= (x^4+6x^2y^2+y^4)h_{31} + 4xy(x^2+y^2)h_{40} + 2xy(x^2+y^2)\sum_{J=0,2,4}f(J)h_{22}^{(J)} \ , \\
\tilde{h}_{40} &= xy(x^2+y^2)h_{31} + (x^4+y^4)h_{40} + x^2y^2\sum_{J=0,2,4}f(J)h_{22}^{(J)} \ , \\
\tilde{h}_{22}^{(J)} &= 2(\delta_{J0} + \tfrac{2}{5}\hat{J})xy(x^2+y^2)h_{31} + 4(\delta_{J0} + \tfrac{2}{5}\hat{J})x^2y^2h_{40} + (x^4+y^4)h_{22}^{(J)} + 4x^2y^2\sum_{L=0,2,4}g_L(J)h_{22}^{(L)} \ , \\
f(0) &= 1 \ , \quad f(2) = 2\sqrt{5}/7 \ , \quad f(4) = \tfrac{6}{7} \ , \quad g_L(J) = \hat{J}\hat{L}\begin{Bmatrix} 2 & 2 & J \\ 2 & 2 & L \end{Bmatrix} \ , \quad \hat{J} = (2J+1)^{1/2} \ .
\end{aligned} \tag{25}$$

Imposing the condition $\tilde{h}_{20} = 0$ together with Eq. (24) determines x and y. The resulting anharmonicity coefficients

$$r_{ij} = \tilde{h}_{ij}/\tilde{h}_{11} \tag{26}$$

now can be directly compared with the results of Sec. II.

IV. NUMERICAL INVESTIGATION OF THE EXPANSION COEFFICIENTS

For the numerical work we used the surface δ interaction[21] (SDI) as a residual interaction among the nucleons. It is defined by

$$\begin{aligned}
V(1,2) &= -4\pi(\chi_s\hat{P}_s + \chi_t\hat{P}_t)\frac{\delta(r_1-R)\delta(r_2-R)}{r_1r_2}\delta(\theta_{12}) \\
&= V_s + V_t \ ,
\end{aligned} \tag{27}$$

where $\hat{P}_s$ and $\hat{P}_t$ are projection operators on singlet and triplet states with χ_s and χ_t being the corresponding strength parameters. The details of its particle-hole and particle-particle matrix elements $G_J(abcd)$ and $F_J(abcd)$ which enter into the boson-expansion coefficients are given in Appendix B.

For the Se isotopes the five proton and five neutron states shown in Fig. 5(a) provide the main

contributions to the phonon (16). The proton Fermi level lies between the $1f_{5/2}$ and the $2p_{3/2}$ states. The neutron Fermi level for the different isotopes is close to the $1g_{9/2}$ level. The single-particle energies are taken from the work of Nilsson *et al.*[22] with the $1g_{9/2}$ and $2d_{5/2}$ neutron states shifted slightly lower to account for the experimentally[23] observed shifting of the subshell closure from $N=40$ to $N=38$. We also included a scaling factor common to all single-particle energies to obtain a higher level density as indicated in experimental work.[24]

In Fig. 6 we compare the amplitudes c_{ab} of all the two-quasiparticle states that contribute to three different types of phonons:
(i) the collective, angular momentum $J=2$ solution of the Tamm-Dancoff (TD) equations for the SDI, i.e., the lowest-lying solution of the eigenvalue equation

$$(E_a+E_b-\omega)c_{ab}=-\sum_{c\geq d}[(1+\delta_{ab})(1+\delta_{cd})]^{-1}[(u_av_bu_cv_d+v_au_bv_cu_d)F_2(abcd) - (u_av_bu_dv_c+v_au_bv_du_c)(-)^{j_c+j_d}F_2(abdc)+(u_au_bu_cu_d+v_av_bv_cv_d)G_2(abcd)]c_{cd}\ , \tag{28}$$

where E_a and E_b denote the quasiparticle energies and F_2 and G_2 are the SDI matrix elements given in Appendix B;

(ii) a schematic quadrupole phonon of the form

$$c_{ab}=(u_av_b+v_au_b)\langle a\|r^2Y_2\|b\rangle/(E_a+E_b-\omega)\ . \tag{29}$$

The dependence on ω is weak as long as it is not close to the two-quasiparticle energies E_a+E_b, and in Fig. 6 we plot the static values for c_{ab} ($\omega=0$):

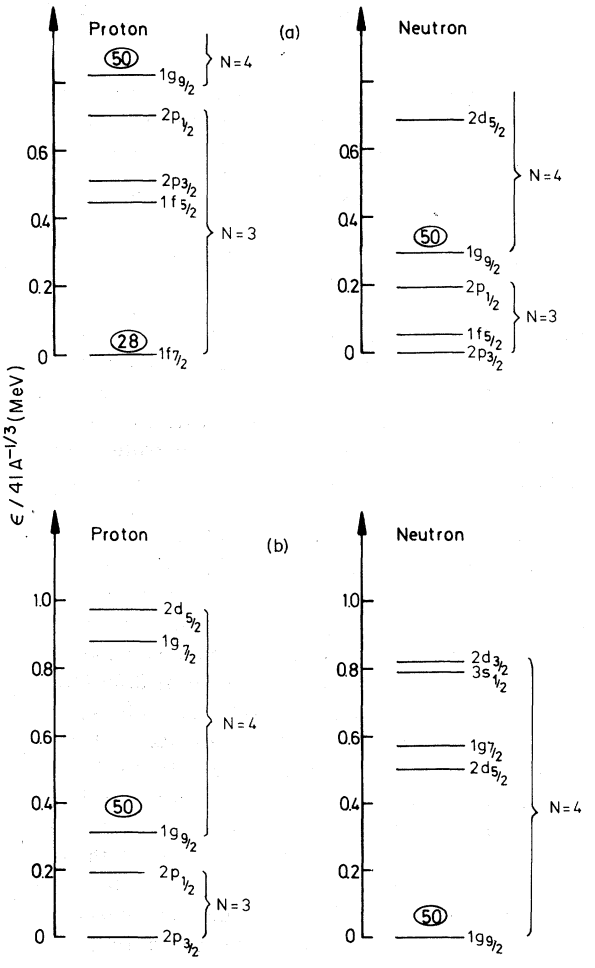

FIG. 5. (a) Single-particle levels in the Se region. (b) Single-particle levels in the Ru region.

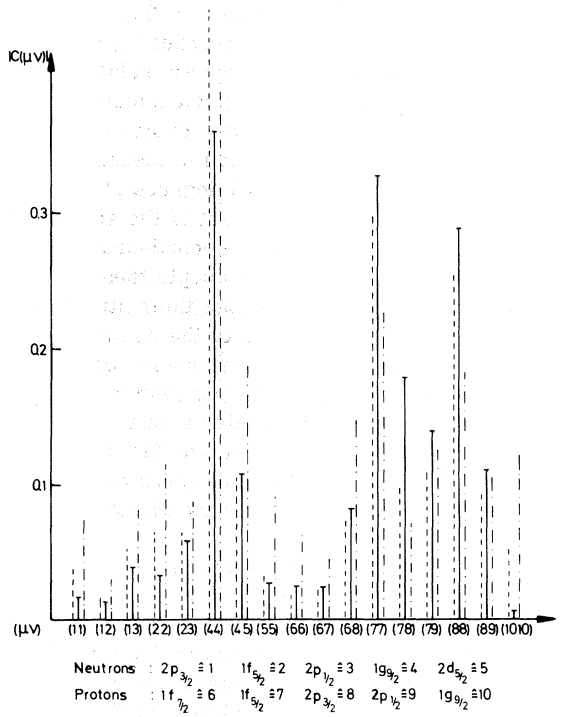

FIG. 6. The phonon-structure amplitudes c_{ab} for three different types of phonons: full lines, collective TD solution for SDI; dashed lines, schematic phonon defined in Eq. (2); and dashed-dotted lines, the two quasiparticle part of the quadrupole operator.

TABLE V. The anharmonicity coefficients r_{ij} calculated for three different types of phonons: (i) collective Tamm-Dancoff solution for SDI; (ii) schematic phonon defined in Eq. (29); (iii) two-quasiparticle part of the quadrupole operator.

	r_{21}	r_{30}	$r_{22}^{(0)}$	$r_{22}^{(2)}$	$r_{22}^{(4)}$	r_{31}	r_{40}
(i)	0.284	0.057	0.243	0.171	0.306	0.420	0.077
(ii)	0.269	0.057	0.241	0.171	0.274	0.396	0.075
(iii)	0.160	0.036	0.268	0.186	0.291	0.398	0.074

(iii) the two-quasiparticle part of the quadrupole operator

$$c_{ab} = (u_a v_b + v_a u_b)\langle a \| r^2 Y_2 \| b \rangle \ . \tag{30}$$

All three phonons display a similar structure with a quite broad distribution among the proton levels and an almost pure single j-shell ($1g_{9/2}$) form of the neutron part. The TD solution is quite close to the schematic phonon (29), while the quadrupole operator leads to more evenly distributed amplitudes.

Evaluating the ratios r_{ij} (26) for these three different types of phonons, we see from Table V that the quadrupole operator phonon (30) leads to marked differences in the third-order r_{21} and r_{30}, while the fourth-order terms remain relatively unaffected by the choice of the phonon structure. Although there is no *a priori* best choice of the phonon operator, the TD solution is distinguished by the fact that it separates all degrees of freedom in the "foreward-going" part of the second order. The "backward-going" second-order term and higher orders might again couple these normal modes to some extent and change their structure, but given all the uncertainties of the configuration space, single-particle energies, choice of residual interaction and its strength parameters, neglect of higher than fourth-order terms, we will restrict ourselves to the collective TD normal mode neglecting the influence of small couplings to other degrees of freedom on the phonon structure.

The difference between the TD energy ω_{TD} and the excitation energy of the first 2^+ state of the full fourth-order Hamiltonian is shown in Figs. 7(a) and 7(b) as functions of the singlet and triplet interaction strength. The corresponding anharmonicity coefficients r_{ij} are plotted in Figs. 8(a)–(c). The singlet parameter χ_s multiplied with the constant radial matrix element I_0 (cf. Appendix B) enters as the pairing force strength into the BCS equations, so we consider for $\chi_s I_0$ values between $17/A$ to $23/A$ (MeV). Keeping $\chi_s I_0$

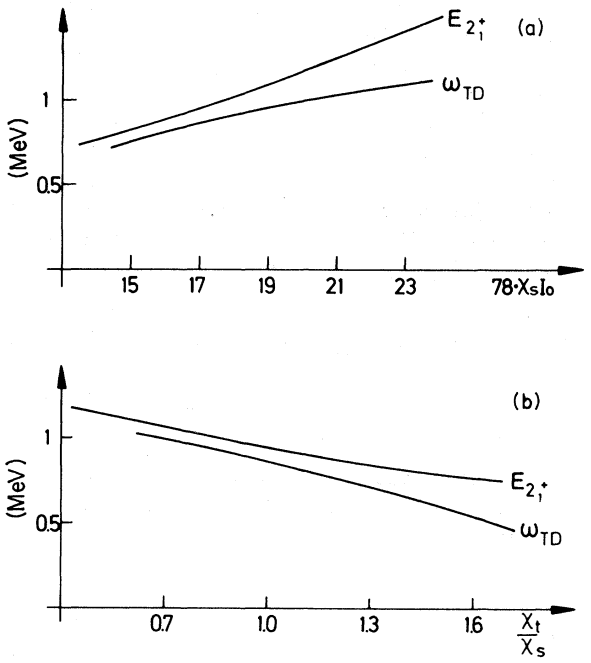

FIG. 7. The collective TD frequency ω_{TD} and the lowest 2^+ eigenvalue of the full collective Hamiltonian as functions of (a) the strength parameter $A\chi_s I_0$, keeping $\chi_s = \chi_t$ and (b) the ratio χ_t/χ_s, keeping $\chi_s I_0 = 17/A$. Both cases are plotted for ^{78}Se with a s.p.e. scaling factor SF = 0.8.

fixed at $17/A$, which is slightly higher than the critical value where the BCS solution collapses and leads to a gap of $\Delta_p = 0.83$, $\Delta_n = 0.97$ for ^{78}Se, the anharmonicities rise steeply with the ratio χ_t/χ_s [Fig. 8(b)]. Therefore the decrease of the first 2^+ energy $E_{2_1^+}$ with increasing χ_t/χ_s is much slower than that of the TD energy ω_{TD} [Fig. 7(b)] and we find it impossible to reach the experimental 2^+ energy of about 0.6 MeV for ^{78}Se. For a scaling factor SF = 0.8 in the single-particle energies (s.p.e.), and $\chi_s = \chi_t = 17/AI_0$ where the anharmonicities are of a magnitude comparable to the fitted values, the 2^+ energy is still at 0.95 MeV.

However, it can be seen from Figs. 8(a)–(c) that the ratios of different coefficients r_{ij} for a given order remain essentially unaffected by changes of χ_s, χ_t/χ_s, and the s.p.e. scaling factor SF. The increase in the pairing strength (even keeping $\chi_s = \chi_t$) leads to a decrease of the third-order anharmonicities [Fig. 8(c)], i.e., to a reduction of the tendency of the nucleus to become deformed. A similar effect has the scaling factor SF on the third-order coefficients, where the "deformation" goes through a maximum at SF = 0.8, and the larger level spacing at SF = 1 as well as

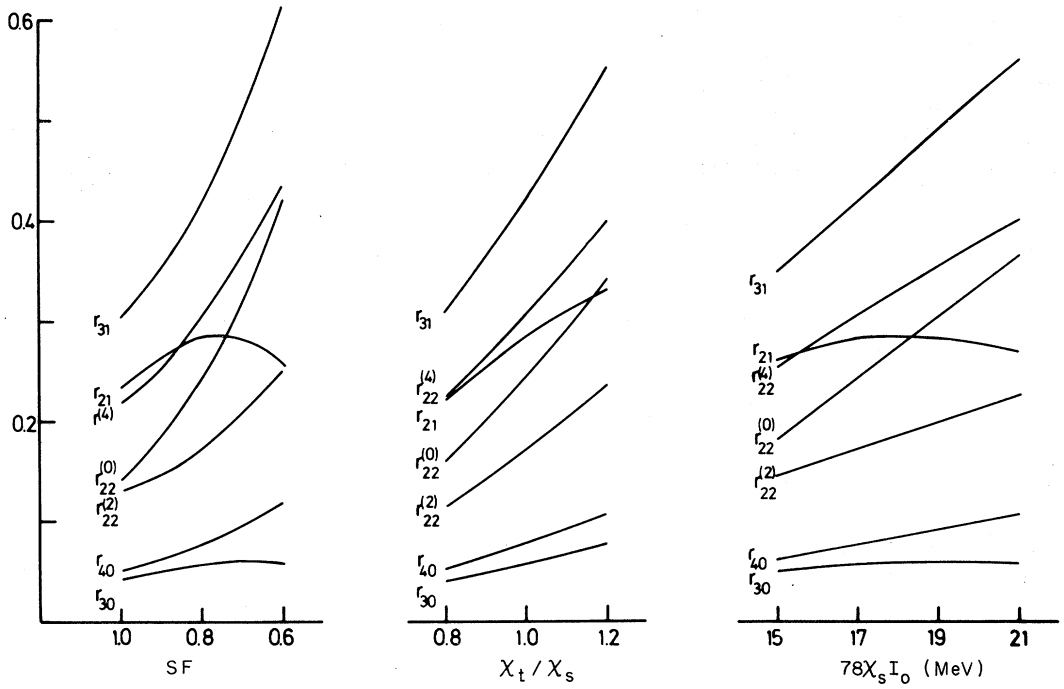

FIG. 8. The anharmonicity coefficients r_{ij} for $A=78$ as functions of (a) the s.p.e. scaling factor SF, for $\chi_s=\chi_t=17/A I_0$, (b) the ratio χ_t/χ_s, with $\chi_s=17/A I_0$, SF = 0.8, and (c) the parameter χ_s, keeping $\chi_s=\chi_t$, SF = 0.8.

the increased gap at higher level density (SF = 0.6) leads to a reduction of the deforming tendency [Fig. 8(a)].

Choosing again $\chi_s=\chi_t=17/AI_0$, SF = 0.8, we show in Fig. 9 the anharmonicities as functions of the neutron number in the Se isotopes. The subshell effect at $N=38$ is markedly pronounced in the third-order coefficients which go through a deep minimum at $N=38$–40. Then with the filling of the $1g_{9/2}$ shell the deformation rises till $N=46$ before it bends down towards the $N=50$ shell closure. The fourth-order anharmonicities decrease almost monotonously as the neutron number comes closer and closer to $N=50$. Similarly, in the Ru isotopes where the neutron number increases beyond $N=50$ [we use the configuration space shown in Fig. 5(b)] there is an almost monotonous rise of the anharmonicity coefficients with the neutron number (Fig. 10). Beyond $N=58$ (approaching the $N=64$ gap in the s.p.e. values) r_{21} decreases again, but for these neutron numbers our configuration space certainly is no longer sufficient. Again we remark that the ratios of coefficients for a given order remain roughly constant for the different isotopes. Average values for the Se isotopes are

$$r_{21}/r_{30}=4.8, \quad r_{31}/r_{40}=5.5\ ,$$
$$r_{22}^{(0)}/r_{40}=3.2, \quad r_{22}^{(2)}/r_{40}=2.1, \quad r_{22}^{(4)}/r_{40}=4.5\ .$$

For the Ru isotopes we have approximately

$$r_{21}/r_{30}=5.1, \quad r_{31}/r_{40}=5.5, \quad r_{22}^{(0)}/r_{40}=3.5,$$
$$r_{22}^{(2)}/r_{40}=2.3, \quad r_{22}^{(4)}/r_{40}=3.5\ .$$

These numbers ought to be compared with the numbers given in Eq. (3). It is satisfying that we find roughly similar relations between the diagonal and off-diagonal coefficients as implied by the simple model leading to Eq. (3) and that these relations seem to be rather stable against variations of all sorts of parameters in the microscopic theory.

The precise values of the coefficients r_{ij} themselves, however, depend sensitively on the position of individual single-particle levels. We have tried to use this freedom to improve the agreement between the calculated coefficients and the numbers obtained in the phenomenological fits from Sec. II. It is interesting to note that interchanging the $1g_{9/2}$ and $2p_{1/2}$ neutron levels (which has been suggested elsewhere[23]) and interchange of the $1f_{5/2}$ and $2p_{3/2}$ proton levels [Fig. 11(a)] leads to almost quantitative agreement for the ^{76}Se and ^{78}Se isotopes (Table VI). In the Ru isotopes with $N=56$ and $N=58$ we simply multiply the Nilsson s.p.e. values with a common scale factor [Fig.11(b)] to obtain the coefficients r_{ij} given in Table VI.

Although the agreement is remarkable, we have

to point out that we always obtain the $r_{22}^{(0)}$ term larger than the fitted value by a factor of up to 1.5 and that we have not been able to obtain the very small $r_{22}^{(2)}$ values which tend to emerge from phenomenological fits. Of course, those fits are not unique and one can try to obtain reasonable fits with larger $r_{22}^{(2)}$ values. For example, the ^{102}Ru fit presented in Sec. II differs from the one given in Ref. 11 by having a $r_{22}^{(2)}$ coefficient which is 0.049 as compared to −0.0535 of the previous $r_{22}^{(2)}$, the quality of the previous[11] fit being slightly better, however, than the present one. Furthermore, the results for ^{78}Kr, ^{80}Kr, and ^{82}Kr contained in Ref. 18 require small negative values for $r_{22}^{(2)}$ which we did not obtain from the microscopic calculation.

Finally, the level schemes depend quite sensitively on the precise values of the coefficients r_{ij}, and, therefore, the agreement shown in Table VI still does not lead to very satisfactory agreement for the energy levels. As an example we repeat in Fig. 12(a) the fitted spectrum for the nucleus ^{100}Ru from Fig. 3. Figure 12(b) then shows the level scheme that results from the microscopically calculated coefficients of Table VI. As we discussed earlier in this section, the energy of the

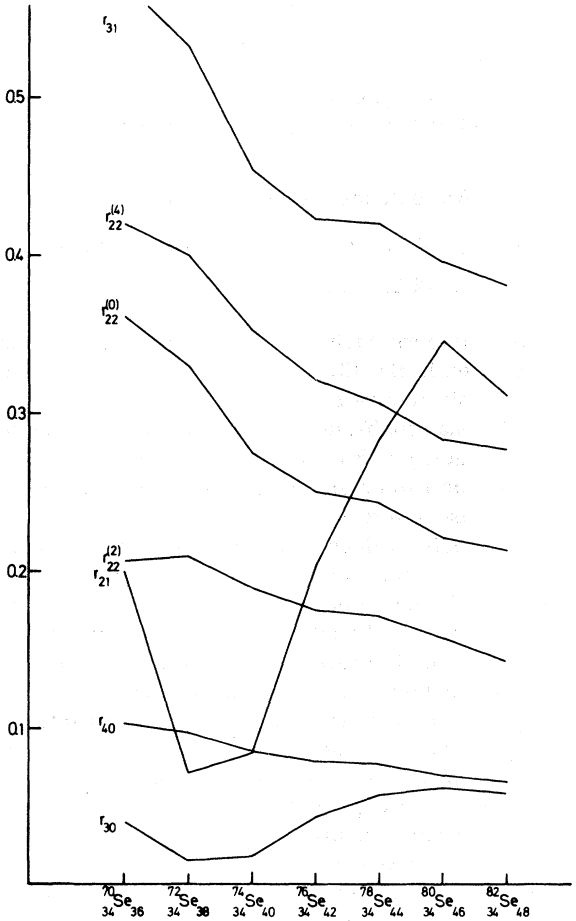

FIG. 9. The anharmonicity coefficients r_{ij} for the Se isotopes as functions of the neutron number ($\chi_s = \chi_t = 17/A\,I_0$, SF = 0.8).

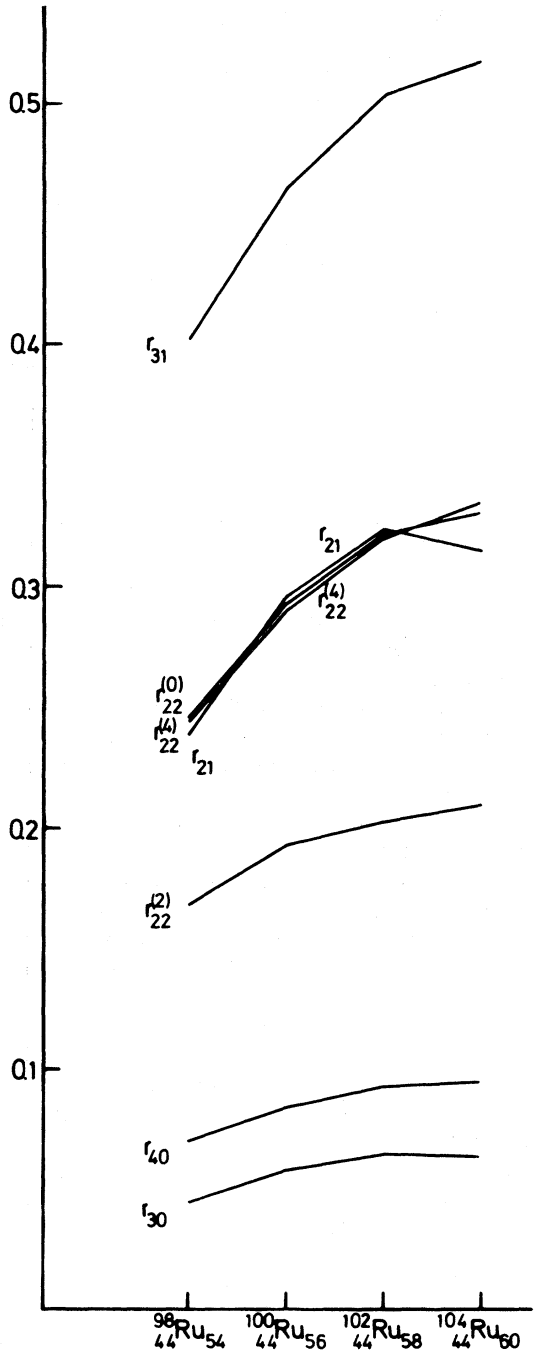

FIG. 10. The anharmonicity coefficients r_{ij} for the Ru isotopes as functions of the neutron number ($\chi_s = \chi_t = 20/A\,I_0$, SF = 0.7).

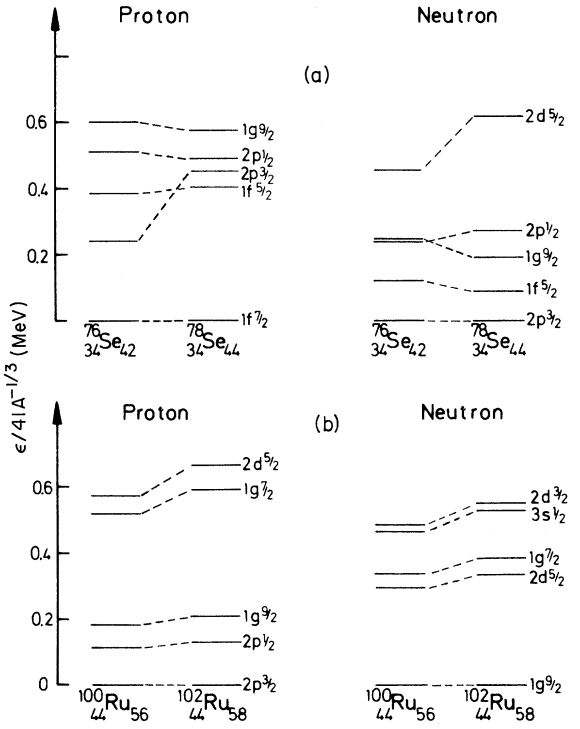

FIG. 11. Adjusted single-particle energies for the isotopes (a) ^{76}Se and ^{78}Se and (b) ^{100}Ru and ^{102}Ru underlying the expansion coefficients r_{ij} given in the rows b of Table VI.

first excited 2^+ state turns out to be too high (by a factor of 1.37 for ^{100}Ru) as compared to the experimental 2^+ level; therefore for this comparison we have normalized the theoretical $\tilde{h}_{11}$ by the inverse of this factor to obtain the 2^+ state at the experimental value. Then we see that the theoretical coefficients give the ground band $(4^+, 6^+)$ with good accuracy, which indicates the insensitivity of these yrast states to the details of the theory. On the other hand, the 0^+ states seem to be the most sensitive, lying much too high. This can be traced directly to the $r_{22}^{(0)}$ coefficient which is larger than $r_{22}^{(0)}$ (fit) by a factor of 1.5. Lowering the value of $r_{22}^{(0)}$, we see in Fig. 12(d) that this has a strong effect on the spectrum and especially on the position of the 0^+ states. Figures 12(c) and 12(e) show the effect of putting r_{30} or $r_{22}^{(2)}$ on their fitted values while keeping all other coefficients fixed at their theoretical values. It seems that the 2^+ and 4^+ members of the triplet remain essentially unaffected by these changes.

Rewriting the collective Hamiltonian in terms of momentum $P \propto i(B^\dagger - B)$ and coordinate $Q \propto (B^\dagger + B)$, we obtain the coefficients ρ^{ij} for the kinetic and potential energy as defined in Eqs. (3) of Ref. 11. For the nuclei discussed here we list the fitted and the theoretical coefficients in Table VII (again with $\tilde{h}_{11}$ normalized as discussed above). The results for the potential (given by ρ^{20}, ρ^{30}, and ρ^{40}) are excellent, while the discrepancies from Table VI seem to enter mainly into the anharmonicities of the kinetic energy terms. For comparison we have included in Figs. 1–4 the theoretical potential energies (in the intrinsic β-γ representation for $\gamma = 0$) to show the similarity of the fitted result with the curve obtained from the boson expansion.

V. CONCLUSION

In this paper we have made an attempt to apply the Marumori boson expansion to nuclei which oscillate around a spherical equilibrium while at the same time the potential energy surface for the collective motion displays a maximum for zero deformation. The basis of the model is an expansion of the collective Hamiltonian in terms of quadrupole boson operators up to fourth order, and we tried to obtain the expansion coefficients on the one hand by fits to experimental level schemes, on the other hand by calculating them on a completely microscopic basis from a modi-

TABLE VI. Comparison for the anharmonicity coefficients r_{ij}: (a) denotes phenomenological fit (cf., Table I) and (b) denotes microscopic calculation with the configuration space of Fig. 11, TD phonons, and SDI.

		r_{21}	r_{30}	$r_{22}^{(0)}$	$r_{22}^{(2)}$	$r_{22}^{(4)}$	r_{31}	r_{40}
^{76}Se	a	0.278	0.062	0.192	0.028	0.375	0.389	0.070
	b	0.272	0.060	0.228	0.165	0.360	0.397	0.073
^{78}Se	a	0.212	0.071	0.277	0.189	0.526	0.605	0.115
	b	0.187	0.041	0.429	0.244	0.448	0.633	0.120
^{100}Ru	a	0.385	0.128	0.254	0.161	0.386	0.580	0.125
	b	0.377	0.080	0.389	0.247	0.384	0.593	0.113
^{102}Ru	a	0.332	0.111	0.237	0.049	0.349	0.480	0.120
	b	0.338	0.069	0.337	0.214	0.336	0.525	0.097

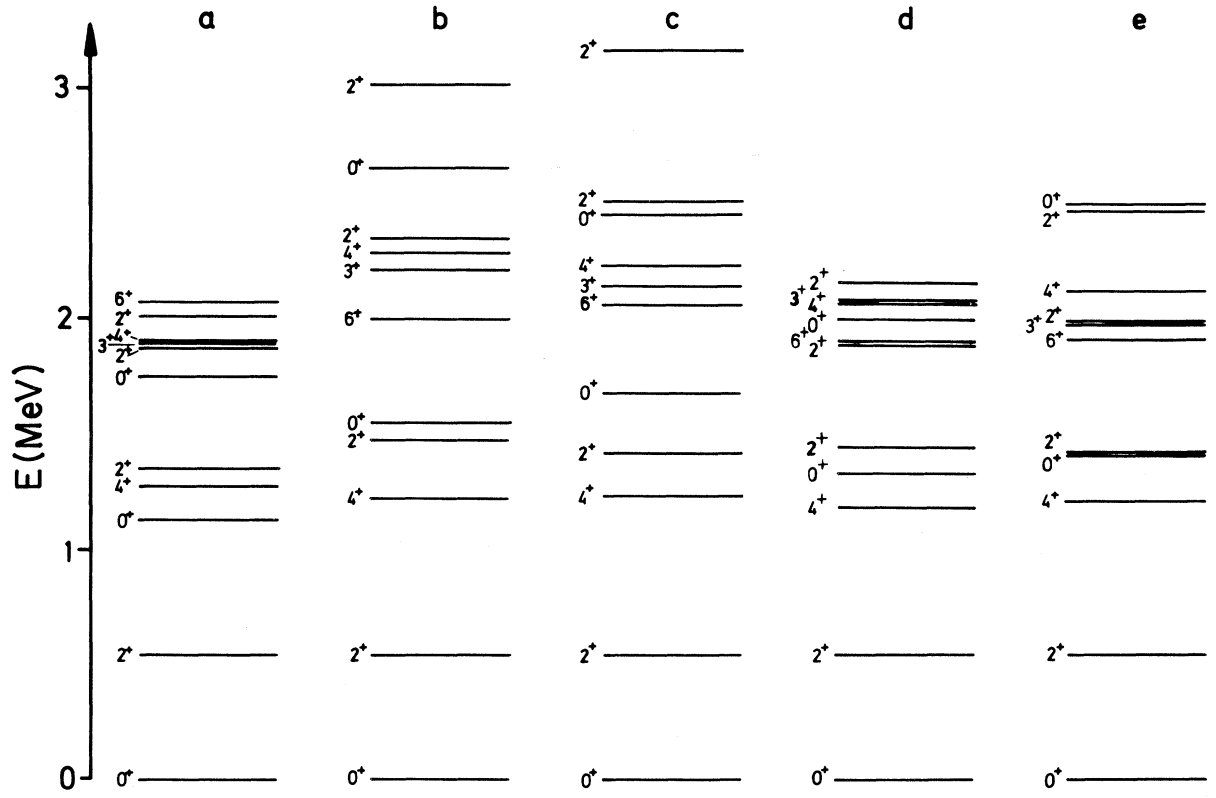

FIG. 12. Calculated level schemes for ^{100}Ru: (a) spectrum resulting from the phenomenological fit (coefficients r_{ij} given in row a of Table VI), (b) spectrum resulting from microscopic theory (coefficients r_{ij} given in row b of Table VI), (c) same as (b) with $r_{30}=0.128$, (d) same as (b) with $r_{22}^{(0)}=0.320$, and (e) same as (b) with $r_{22}^{(2)}=0.161$.

fied Marumori approach.

There are several ambiguities in such an attempt: The most severe seems to be the restriction of the expansion to the fourth-order. By fitting a fourth-order Hamiltonian to a given energy spectrum, one might renormalize the effects of terms higher than fourth order into the low-order coefficients. It therefore seems doubtful whether a comparison with theoretical third and fourth-order terms is justified. This might well be a reason for discrepancies which we found for the $r_{22}^{(0)}$ and $r_{22}^{(2)}$ coefficients. However, for the nuclei considered here, which are essentially spherical with still rather small amplitudes of the collective motion, we think that the fifth- and sixth-order terms should be unimportant. Furthermore, in

TABLE VII. The coefficients ρ^{ij} for kinetic and potential energy [cf. Eqs. (3) of Ref. 11]: (a) denotes phenomenological fit, and (b) denotes microscopic calculation with the configuration space of Fig. 11, TD phonons, and SDI.

		ρ^{20}	ρ^{30}	ρ^{40}	ρ^{22}	ρ^{32}	ρ_0^{42}	ρ_2^{42}	ρ_4^{42}	ρ^{44}
^{76}Se	a	−0.556	0.131	0.139	1.516	0.142	0.062	0.112	−0.109	−0.164
	b	−0.642	0.123	0.146	1.098	0.137	0.088	0.042	−0.046	−0.010
^{78}Se	a	−1.212	0.117	0.237	1.413	0.000	0.129	0.073	−0.127	−0.214
	b	−1.248	0.093	0.252	1.477	0.104	0.067	0.067	−0.008	−0.092
^{100}Ru	a	−1.133	0.242	0.248	2.323	0.002	0.049	0.032	−0.117	−0.418
	b	−1.102	0.185	0.231	1.583	0.219	0.054	0.034	0.006	−0.133
^{102}Ru	a	−0.655	0.166	0.165	1.879	0.0	−0.005	0.073	−0.114	−0.228
	b	−0.776	0.139	0.171	1.383	0.177	0.041	0.028	0.003	−0.129

principle the fourth-order Hamiltonian already requires a seven-parameter fit, and with often incomplete experimental information it is difficult to find a true minimum in the seven-dimensional parameter space. Higher orders introduce too much freedom for a meaningful model.

Naturally, the microscopic approach contains a number of ambiguities of different kinds. As usual, one has to deal with the uncertainties of single-particle levels, two-body interaction, and the truncations of the configuration space. A question in principle is the choice of the phonon operator which is used as a basis for the expansion. We made use of the collective Tamm-Dancoff solution because it separates the degrees of freedom at least in the lowest order (which is by far the largest term). Then there is the problem of choosing among at least three different expansion techniques. Marshalek's remark[25] about this in mind, we follow here our appreciation of Marumori's method, with slight modifications brought about by the truncation to the subspace of collective phonons.

Despite all these ambiguities we have found a remarkable agreement for the ratios of anharmonicity coefficients with the fitted values. These ratios seem to be rather insensitive to the details of the microscopic theory and are not too different from the results of a very simple $P^2/2M + V(Q)$ model. For two of the diagonal fourth-order coefficients we found more serious discrepancies with the fitted values which we could not resolve up to now. Comparing with the above-mentioned $P^2/2M + V(Q)$ results [Eq. (3)], however, we have the feeling that the trouble is not necessarily with the Marumori expansion but possibly with the fitted coefficients [especially in case of $r_{22}^{(2)}$ which often differs strongly from Eq. (3)]. The 0^+ states are mainly affected by these coefficients and it seems that the small $r_{22}^{(0)}$ and $r_{22}^{(2)}$ values needed to bring them down to their low experimental positions try to make up for a different physical mechanism which is not contained in the quadrupole phonon approach. Another hint in that direction is provided by the extremely low-lying 0^+ states at subshell closure, which cannot be satisfactorily described by the phonon model alone, but indicate further coupling to other degrees of freedom (especially to pairing vibrations[26]). Such couplings seem to be more important[27] than including higher-order terms into a pure quadrupole-phonon Hamiltonian.

The boson-expansion approach discussed here complements the ATDHF method[28] in the sense that for smaller amplitudes around the spherical shape (which, however, go beyond a harmonic approximation) it supplies a genuinely quantum-mechanical description with the collective mode being at least partly determined by the microscopic dynamics, without any classical steps. It does not make assumptions about the form of the kinetic energy of the collective Hamiltonian. For genuine large amplitude collective motion, however, the ATDHF method seems superior by the ease with which it takes the deformation of the underlying fermion basis into account, while in the boson expansion the structure of the phonon is fixed; in our case it is always expressed in terms of single-particle states in a spherical basis.

One of us (GH) would like to thank Dr. T. Kishimoto for helpful correspondence.

APPENDIX A

We present here the explicit expressions for the normalization constants N_n^F and N_n^B defined in Eqs. (15) and the boson-expansion coefficients h_{ij} from Eqs. (22). The boson-normalization constants are

$$N_1^B = 1 ,$$

$$N_{2J}^B = \frac{1}{\sqrt{2!}} , \quad J = 0, 2, 4 ,$$

$$N_{3(J)}^B = \left(2 \left[1 + 2(2J+1) \begin{Bmatrix} 2 & 2 & J \\ 2 & 2 & J \end{Bmatrix} \right] \right)^{-1/2} .$$

The Fermi normalization constants are

$$N_1^F = \left(2 \sum_{ab} c_{ab} c_{ab} \right)^{-1/2} = 1 ,$$

$$N_{2J}^F = \frac{1}{\sqrt{2!}} \left(1 - 200 \sum_{a-d} c_{ab} c_{cd} c_{ac} c_{bd} \begin{Bmatrix} j_a & j_b & 2 \\ j_c & j_d & 2 \\ 2 & 2 & J \end{Bmatrix} \right)^{-1/2} ,$$

$$N^F_{3(J)} = \Bigg\{ 2 \sum_{K=0,2,4} \left(\delta_{KJ} + 2\hat{J}\hat{K} \begin{Bmatrix} 2 & 2 & J \\ 2 & 2 & K \end{Bmatrix} \right) \Bigg[\delta_{KJ} - 400 \left(\delta_{KJ} + 2\hat{J}\hat{K} \begin{Bmatrix} 2 & 2 & J \\ 2 & 2 & K \end{Bmatrix} \right) \sum_{a-d} c_{ab} c_{cd} c_{ac} c_{bd} \begin{Bmatrix} j_a & j_b & 2 \\ j_c & j_d & 2 \\ 2 & 2 & K \end{Bmatrix}$$

$$+ 8000 \hat{J}\hat{K} \sum_{a-f} c_{ab} c_{ac} c_{be} c_{cd} c_{df} c_{ef} \sum_{jj'} (-)^{j'} (2j+1)(2j'+1)$$

$$\times \begin{Bmatrix} 2 & j' & K \\ 2 & 2 & j \end{Bmatrix} \begin{Bmatrix} 2 & 2 & J \\ 2 & 2 & j \end{Bmatrix} \begin{Bmatrix} j_a & j_b & 2 \\ j_c & j_e & j' \\ 2 & 2 & K \end{Bmatrix} \begin{Bmatrix} j_c & j_d & 2 \\ j_e & j_f & 2 \\ j' & 2 & j \end{Bmatrix} \Bigg] \Bigg\}^{-1/2} ,$$

$\hat{J} = (2J+1)^{1/2}$.

The normalization constants for the three-phonon states satisfy the relations

$$\frac{N^B_{30}}{N^B_{3J}} = \frac{N^F_{30}}{N^F_{3J}} = \frac{2(2J+1)^{1/2}}{7}, \quad J = 2, 4 .$$

The expansion coefficients h_{ij} are given by

$$h_{11} = 2\sqrt{5}\, N_1^{F^2} \left\{ \sum_{ab} (E_a + E_b) c_{ab} c_{ab} + \tfrac{1}{2} \sum_{a-d} [G_2(ab, cd)(u_a u_b u_c u_d + v_a v_b v_c v_d) + 4 F_2(ab, cd)(u_a u_c v_b v_d) c_{ab} c_{cd}] \right\} ,$$

$$h_{20} = -\sqrt{10}\, N^F_{20} \sum_{a-d} [G_2(ab, cd) u_a u_b v_c v_d - 2F_2(ab, cd) u_a u_d v_b v_c]\, c_{ab} c_{cd} ,$$

$$h_{21} = 20\sqrt{10}\, N^F_{22} N^F_1 \sum_{a-e} [G_2(ab, cd)(u_a u_b u_d v_c - v_a v_b v_d u_c)$$

$$+ 2F_2(ab, cd)(u_a v_b v_c v_d - v_a u_b u_c u_d)]\, c_{ab} c_{ec} c_{de} \begin{Bmatrix} 2 & j_c & j_d \\ j_e & 2 & 2 \end{Bmatrix} ,$$

$$\delta_{KJ} = \sqrt{\tfrac{5}{14}}\, h_{310} + \sqrt{5} \left(\frac{N^B_{20}}{N^F_{20}} \frac{N^F_{30}}{N^B_{30}} - 1 \right) h_{20} ,$$

$$h_{31J} = -200 N^F_{3J} N^F_1 \sum_{K=0,2,4} \hat{K} \left(\delta_{KJ} + 2\hat{K}\hat{J} \begin{Bmatrix} 2 & 2 & J \\ 2 & 2 & K \end{Bmatrix} \right)$$

$$\times \sum_{a-f} \Bigg((-)^{j_a + j_b + j_c + j_d} [4 F_2(ab, cd) u_b u_c v_a v_d + G_2(ab, cd) u_a u_b v_c v_d]$$

$$\times \begin{Bmatrix} K & j_d & j_e \\ j_c & 2 & 2 \end{Bmatrix} \begin{Bmatrix} K & j_d & j_e \\ j_f & 2 & 2 \end{Bmatrix} - G_2(ab, cd) u_c u_d v_a v_b \begin{Bmatrix} j_c & j_d & 2 \\ j_e & j_f & 2 \\ 2 & 2 & K \end{Bmatrix} \Bigg) c_{ab} c_{ce} c_{df} c_{ef} ,$$

$$h^{(J)}_{22} = h^{(J)'}_{22} + \frac{\hat{J}}{\sqrt{5}} \left[\left(\frac{N^F_{2J}}{N^B_{2J}} \right)^2 - 1 \right] h_{11} ,$$

$$h_{22}^{(J)\gamma} = -400\hat{J}N_{2J}^{F\,2}\Bigg(\sum_{a-d}(E_a+E_b)\,c_{ab}c_{cd}\,c_{ac}c_{bd}\begin{Bmatrix} j_a & j_b & 2\\ j_c & j_d & 2\\ 2 & 2 & J\end{Bmatrix}\cdot$$

$$+\sum_{a-f}[G_2(ab,cd)(u_au_bu_cu_d+v_av_bv_cv_d)+4F_2(ab,cd)u_au_cv_bv_d]\begin{Bmatrix} j_a & j_b & 2\\ j_e & j_f & 2\\ 2 & 2 & J\end{Bmatrix}c_{ae}c_{bf}c_{cd}c_{ef}$$

$$-\sum_{a-f}\sum_{L}\{G_L(ab,cd)(u_au_bu_cu_d+v_av_bv_cv_d)+2[F_L(ab,cd)u_au_cv_bv_d$$

$$-(-)^{j_a+j_b+L}F_L(ba,cd)u_bu_cv_av_d]\}c_{ae}c_{bf}c_{ce}c_{df}\sum_j(2j+1)\begin{Bmatrix} j_a & j_b & L\\ j_e & j_d & j\\ 2 & 2 & J\end{Bmatrix}\begin{Bmatrix} j_c & j_d & L\\ j_e & j_f & j\\ 2 & 2 & J\end{Bmatrix}\Bigg)$$

$$h_{30}=h_{40}=0\ .$$

The quantities u_a and v_a denote the BCS amplitudes; the particle-particle and particle-hole matrix elements G_J and F_J are defined by

$$\langle\alpha\beta\,|\,V\,|\,\gamma\delta\rangle=\sum_{JM}G_J(ab,cd)(j_am_aj_bm_b|JM)(j_cm_cj_dm_d|JM)$$

$$=\sum_{JM}F_J(ab,cd)(-)^{j_c-m_c}(j_am_aj_c-m_c|JM)(-)^{j_b-m_b}(j_dm_dj_b-m_b|JM)$$

and are given for the SDI in Appendix B.

APPENDIX B

The SDI particle-particle matrix element for proton pairs or neutron pairs are

$$G_J(abcd)=\langle abJ\,|\,V_s\,|\,cdJ\rangle_{\rm AS}$$

$$=2(-)^{l_a+l_c}\chi_s[1+(-)^{l_a+l_b+J}]M(abcd,J)\ .$$

Particle-hole matrix elements for protons $\langle(pp^{-1})|V|(pp^{-1})\rangle$ or neutrons $\langle(nn^{-1})|V|(nn^{-1})\rangle$ are

$$F_J(abcd)=\langle ab^{-1}J\,|\,V_s\,|\,cd^{-1}J\rangle_{\rm AS}$$

$$=2\chi_s[(-)^{l_a+l_b+J}M(abcd,J)-N(abcd,J)]\ .$$

Particle-hole matrix elements for neutron-particle–neutron-hole and proton-particle–proton-hole $\langle(nn^{-1})|V|(pp^{-1})\rangle$ are

$$F_J(abcd)=\langle ab^{-1}J\,|\,V\,|\,cd^{-1}J\rangle_{\rm AS}$$

$$=[(\chi_t+\chi_s)(-)^{l_a+l_b+J}+2\chi_t]M(abcd,J)$$

$$+(\chi_t-\chi_s)N(abcd,J)\ .$$

AS denotes antisymmetrization and we have

$$M(abcd,J)=-\frac{1}{4(2J+1)}I_0$$

$$\times\prod_{i=a-d}\hat{j}_i(-)^{j_a+j_c+1}C^{j_a\,j_b\,J}_{\frac12-\frac12\,0}C^{j_c\,j_d\,J}_{\frac12-\frac12\,0}\ ,$$

$$N(abcd,J)=-\frac{1}{4(2J+1)}I_0$$

$$\times\prod_{i=a-d}\hat{j}_i(-)^{l_a+l_c}C^{j_b\,j_a\,J}_{\frac12\,\frac12\,1}C^{j_d\,j_c\,J}_{\frac12\,\frac12\,1}$$

$$[\hat{j}=(2j+1)^{1/2}]\ .$$

The radial integrals I_0

$$I_0=\psi^*_{i_a}(R)\psi^*_{i_b}(R)\psi_{l_c}(R)\psi_{i_d}(R)R^2$$

have been as usual approximated by the same constant for all different states.

[1]A. Bohr, K. Dan. Vidensk. Selsk. Mat.-Fys. Medd. 26, No. 14 (1952).
[2]E. Eichler, Rev. Mod. Phys. 36, 809 (1964).
[3]H. Schmidt, Z. Phys. 181, 532 (1964); D. R. Bés and R. A. Broglia, Nucl. Phys. 80, 289 (1966).
[4]G. Holzwarth, Nucl. Phys. A156, 511 (1970).
[5]G. Holzwarth, Nucl. Phys. A174, 97 (1971).
[6]G. Gneuss and W. Greiner, Nucl. Phys. A171, 449 (1971).
[7]D. M. Brink, A. F. R. De Toledo Piza, and A. K. Kerman, Phys. Lett. 19, 413 (1965).
[8]T. K. Das, R. M. Dreizler and A. Klein, Phys. Rev. C 2, 632 (1970).
[9]J. Hadermann and A. C. Rester, Nucl. Phys. A231, 120 (1974); F. Jachello and A. Arima, Phys. Lett. 53B, 309 (1974).
[10]A. K. Kermann and C. M. Shakin, Phys. Lett. 1, 151 (1962).
[11]G. Holzwarth and S. G. Lie, Z. Phys. 249, 332 (1972).
[12]D. Habs *et al.*, Z. Phys. 267, 149 (1974).
[13]S. T. Belyaev and V. G. Zelevinsky, Nucl. Phys. 30, 582 (1962).
[14]T. Marumori, M. Yamamura, and A. Tokunaga, Prog. Theor. Phys. 31, 1009 (1964).
[15]B. Sørensen, Nucl. Phys. A97, 1 (1967); A119, 65 (1968); A142, 392, 411 (1970).
[16]M. Kleber, Phys. Lett. 30B, 588 (1969).
[17]S. C. Pang, A. Klein, and R. M. Dreizler, Ann. Phys. (N.Y.) 49, 477 (1968).
[18]G. Holzwarth and S. G. Lie, in Proceedings of the Topical Meeting on Vibrational Nuclei, Zagreb 1974 (unpublished).
[19]D. Janssen (private communication).
[20]E. R. Marshalek and G. Holzwarth, Nucl. Phys. A191, 438 (1972); D. Janssen *et al.*, *ibid.* A172, 142 (1972).
[21]I. M. Green and S. A. Moszkowski, Phys. Rev. 139, 79 (1965).
[22]S. G. Nilsson *et al.*, Nucl. Phys. A131, 1 (1969).
[23]N. Kato, Nucl. Phys. A203, 97 (1973); E. Nolte *et al.*, Z. Phys. 268, 267 (1974).
[24]R. Broda *et al.*, Nucl. Phys. A216, 493 (1973).
[25]E. Marshalek, in *Proceedings of the International Conference on Nuclear Moments and Nuclear Structure, Osaka, 1972*, edited by H. Horie and K. Sugimoto, [J. Phys. Soc. Jpn. Suppl. 34, 405 (1973)].
[26]B. Sørensen, Nucl. Phys. A177, 465 (1971).
[27]T. Kishimoto and T. Tamura, in Proceedings of the International Conference on Nuclear Moments and Nuclear Structure, Osaka, 1972, edited by H. Horie and K. Sugimoto (see Ref. 25), p. 393.
[28]M. Baranger and K. Kumar, Nucl. Phys. A122, 241 (1968).
[29]M. Sakai, University of Tokyo Report No. INS-J-142, July, 1973 (unpublished).
[30]D. Rabenstein and H. Vonach, Z. Naturforsch. 3, 458 (1971).
[31]B. Singh and H. W. Taylor, Nucl. Phys. A155, 70 (1970).
[32]H. Ikegami, W. B. Ewbank, and K. Way, Nucl. Data B1 (No. 6), 120 (1966); D. C. Kocher, Nucl. Data Sheets B11, 304 (1974).
[33]F. K. McGowan *et al.*, Nucl. Phys. A113, 529 (1968).